Korean J. Chem. Eng., **31**(9), 1681-1694 (2014)
DOI: 10.1007/s11814-014-0102-7

pISSN: 0256-1115
eISSN: 1975-7220

Rheological characterization of ferrous sulfate-containing water-in-oil-in-water ($W_1/O/W_2$) double emulsions

Mozhgan Keyvani, Leila Davarpanah, and Farzaneh Vahabzadeh†

Chemical Engineering Department, Amirkabir University of Technology (Tehran Polytechnic), 424 Hafez Ave, Tehran, Iran
(*Received 10 September 2013 • accepted 8 April 2014*)

Abstract−With use of response surface methodology (RSM), the $W_1/O/W_2$ emulsions containing ferrous sulfate as the inner phase were optimized in terms of stability (ES) and apparent viscosity (μ_{app}). Curvature display of the responses around their optimal settings was appropriately described using the quadratic polynomial regression model. The non-Newtonian behavior of the test $W_1/O/W_2$ emulsions was characterized using the power-law model and change from non-Newtonian to Newtonian ($n \simeq 1$) was seen in the case of $W_1/O : W_2$ ratio equal 20 : 80 when the level of Tween-80 was 1 v%. Results of the size distribution pattern showed 60% of the particles were less than 5 μm. Rheological properties of the test $W_1/O/W_2$ emulsions as the viscoelastic liquids were analyzed and the results of oscillatory experiments considering shear stress and frequency dependency of G′ and G″ moduli were discussed in terms of the internal microstructure of the emulsions.

Keywords: $W_1/O/W_2$ Double Emulsions, Statistical Design, Power-law Model, Viscoelastic Properties, Tween-80

INTRODUCTION

Water-in-oil-in-water ($W_1/O/W_2$) emulsions are examples of multi-compartmentalized systems where minute water particles (W_1) inside fat droplets (O) themselves act as emulsion being dispersed in a continuous aqueous phase (W_2) [1]. Capability of double emulsion technology to entrap or encapsulate a test compound in its internal compartment has made this technology a suitable method for several situations, particularly for food and pharmaceutical areas. Reduction in intake of fat (calorie) and salt, and improvement in intake of vitamins, amino acids, phenolics, microorganisms (lactic acid producing bacteria), and minerals such as iron are some examples in foods [2-4]. While, availability of some bioactive compounds such as parenteral nutritional materials could substantially be improved with use of the double emulsion technology [5]. Further advantages of using this technology are because of the controlled release of the encapsulated material under the specified condition. This character has extended the application of the multiple emulsions to non-food and non-pharmaceutical areas (such as slow release of fertilizers and pesticides for agricultural uses) [5].

The point of interest in the area of emulsion formation is to focus on kinetic stability since thermodynamic stability does not give any indication of the time-dependency of the physicochemical changes which occur in emulsion's properties. The thermodynamically unfavorable process of emulsion formation actually is due to involvement of hydrophobic effect when a mixture of two immiscible liquids is prepared. Increase in the contact area between two liquids (ΔA) is through the interfacial energy ($\Delta G_I = \gamma \Delta A$), where γ is a proportionality constant called the interfacial tension [1]. Contribution of ΔG_I in the total free energy change of the emulsion formation ($\Delta G_{total} = \gamma \Delta A - T\Delta S$) has a determining role in defining thermodynamically stable or unstable emulsions. Dominance of $-T\Delta S$ term at the low levels of $\gamma \Delta A$ in determination of ΔG_{total} results in formation of micro-emulsions which are thermodynamically stable colloidal solutions [6].

Because of simultaneous presence of the two thermodynamically unstable interfaces in the double emulsions, these colloidal solutions are highly sensitive to variations of individual components used in the preparation of macroemulsions [7]. Selection of the lipophilic surfactant for the W_1/O primary emulsion of the $W_1/O/W_2$ system is usually carried out in the same way as is used for the stabilization of the interface of the single W/O emulsions, while stabilization of the second interface in the $W_1/O/W_2$ emulsions is more critical in terms of the hydrophilic surfactant selection [7,8]. Obtaining optimal HLB value when two different surfactants having two different HLB values are used is possible, and the shift of this value at different emulsifier concentrations has found to be a result of the excess hydrophobic emulsifier present in the oil phase [8]. Apparently, the ideal HLB value for hydrophilic emulsifiers (the surfactant used for the W_2 aqueous in the $W_1/O/W_2$ system) increases when the amount of this surfactant is lowered [8].

Importance of rheological studies in terms of interactions between surfactants and proteins has been studied, where protein binding abilities of Tweens as non-ionic surfactants are low and these emulsifiers are weak protein binders, so they are less influential on the rheological properties of the system [9].

Study on interaction between sodium dodecyl sulphate (SDS) anionic surfactant and bovine β-lactoglobulin has shown that increasing surfactant concentration increased the net negative charge on the surfactant-protein complex (increase in negative zeta potential of emulsion droplets as a function of surfactant concentration) [10]. Thus, use of Tweens in foods and pharmaceutical industry is preferred in comparison with the use of lecithin which is a zwitterionic surfactant. The interactions between the ionic surfactant and proteins significantly affect the rheological characters of the system

†To whom correspondence should be addressed.
E-mail: far@aut.ac.ir

under study [9].

The Pickering emulsions in which the finely divided solids perform as emulsifiers have gained popularity in recent years [11,12]. Certain natural substances such as enzymatically produced starch derivatives (cyclodextrins) are found to have capacity to form complexes with organic compounds, and the resulting complexes in emulsions behave similarly as those of the solid particles [13].

Gain of information about the flow behavior of emulsions is decisive in use of (multiple) emulsion technology in the relevant industries (food, pharmaceutical, agriculture, and environmental). One approach in the characterization of a test system rheology is to obtain viscosity as a function of shear rate. The type of viscosity dependency on shear rate is used for Newtonian/non-Newtonian fluid characterization. Power-law, Bingham, and Casson are the most fre-

Table 1. The four independent variables and their selected levels used in the present study to evaluate $W_1/O/W_2$ characteristics in terms of the emulsion stability (ES) (y_1, '$abs_{650\ nm}$') and the apparent viscosity (μ_{app}) (y_2, 'cP') (a). Arrangement of the 2^4 FCCCD is also shown (b)

(a)

Independent variables	Range and levels of variables (coded)		
	−1	0	+1
x_1: W_1/O : W_2 ratio (v : v%)	30 : 70	20 : 80	10 : 90
x_2: Twee- 80 concentration (v%)	0.5	1	1.5
x_3: Time of homogenization (min)	4	6	8
x_4: Speed of homogenizer (rpm)	8000	11500	15000

(b)

Experimental run numbers	Coded levels				Responses			
	x_1	x_2	x_3	x_4	y_1	$\hat{y}_1^*$	y_2	$\hat{y}_2^*$
1	−1	−1	−1	−1	0.65	0.66	2.23	2.08
2	+1	−1	−1	−1	0.42	0.42	1.69	1.75
3	−1	+1	−1	−1	0.75	0.75	0.85	1.17
4	+1	+1	−1	−1	0.39	0.37	1.68	1.52
5	−1	−1	+1	−1	0.52	0.50	4.11	4.09
6	+1	−1	+1	−1	0.24	0.26	1.51	1.40
7	−1	+1	+1	−1	0.58	0.59	3.63	3.79
8	+1	+1	+1	−1	0.20	0.21	1.79	1.78
9	−1	−1	−1	+1	0.60	0.64	3.32	3.31
10	+1	−1	−1	+1	0.23	0.22	3.01	2.97
11	−1	+1	−1	+1	0.84	0.82	2.67	2.40
12	+1	+1	−1	+1	0.27	0.26	2.51	2.74
13	−1	−1	+1	+1	0.77	0.74	4.06	3.97
14	+1	−1	+1	+1	0.32	0.32	1.25	1.28
15	−1	+1	+1	+1	0.91	0.92	3.90	3.68
16	+1	+1	+1	+1	0.32	0.35	1.53	1.67
17	−1	0	0	0	0.85	0.86	2.31	2.53
18	+1	0	0	0	0.47	0.46	1.56	1.35
19	0	−1	0	0	0.47	0.47	2.52	2.85
20	0	+1	0	0	0.56	0.53	2.79	2.59
21	0	0	−1	0	0.65	0.68	1.45	1.46
22	0	0	+1	0	0.63	0.65	1.80	1.92
23	0	0	0	−1	0.62	0.63	1.94	1.66
24	0	0	0	+1	0.66	0.69	2.16	2.22
25	0	0	0	0	0.67	0.66	1.86	1.94
26	0	0	0	0	0.64	0.66	1.83	1.94
27	0	0	0	0	0.67	0.66	2.09	1.94
28	0	0	0	0	0.69	0.66	2.01	1.94
29	0	0	0	0	0.70	0.66	1.70	1.94
30	0	0	0	0	0.69	0.66	2.07	1.94

*The predicted responses ($\hat{y}_1$ and $\hat{y}_2$) obtained using the quadratic regression equation after analyzing the model ANOVAs according to the summary statistics given in Table 2

quently used models to describe quantitatively the rheological properties of a test fluid such as emulsion [14]. Multiple emulsions as the viscoelastic materials exhibit characteristics of both liquids and solids, and analysis of the rheological properties of these systems on basis of oscillatory experiments provides good information about the emulsion internal microstructure thus its stability [15,16].

In study on use of double emulsions in preparing edible films intended to be used in food industry, rheological, mechanical, and water-vapor properties of these films have been found to be crucial in describing their microstructure and barriers [17]. Besides these, entrapment of material such as iron, which is considered as one of the major pro-oxidants in foods, could be an efficient way to physically separate it from oxidatively unstable lipid substrate (i.e., iron as the inner phase of the $W_1/O/W_2$ emulsions). The double emulsion technology also can be used to reduce the extent of iron deficiency as one of the principal public health problems [3].

With considering all these facts, preparing $W_1/O/W_2$ emulsions with iron as the inner phase was the objective of the present work. The point of interest was to evaluate viscosity and stability of these emulsions under influence of some selected factors which were used in statistical optimization of the double emulsions. These variables were $W_1/O : W_2$ ratio, Tween-80 concentration, and time and speed of homogenization and response surface methodology (RSM) have been used in these optimizations.

Test double emulsions were prepared with incorporation of ferrous sulfate in the internal aqueous phase of the W_1/O, where the corn oil was used as the oil phase. The preparation of the $W_1/O/W_2$ double emulsions in the present study was based on use of two emulsifier procedure, Span-80 and Tween-80, as the two non-ionic emulsifiers having, respectively, low- and high-HLB value.

Power law, Bingham, and Casson models were used to quantitatively characterize the non-Newtonian behavior of the test $W_1/O/W_2$ emulsions. Emulsion shear rate dependency of apparent viscosity (μ_{app}) of these emulsions was also analyzed in terms of the dispersed phase volume fraction and Tween-80 concentration. Further work was to study the viscoelastic properties with use of oscillatory measurements.

EXPERIMENTAL

1. Materials

All the materials and reagents used in the present study were of analytical grade (Merck and Sigma Aldrich) purchased from local suppliers.

2. Emulsion Preparation

The $W_1/O/W_2$ double emulsions were prepared at room temperature using two-step emulsification procedure in which two surfactants were used: Tween-80 having HLB=15 and Span-80 with HLB of 4.3 [18]. In the first stage, Span-80 surfactant was used in W_1/O emulsion preparation, where 10 v% of the surfactant was added to 90 v% corn oil. The mixture was homogenized for 10 min with a magnetic stirrer. The inner aqueous phase contained $FeSO_4 \cdot 7H_2O$ and ascorbic acid at concentrations of (v%) 2 and 1.33 in distilled water, respectively. This aqueous phase was added dropwise to the oil phase using a HO4 Edmund Buhler 7400 Tubingen homogenizer (Germany) with 10:90 ratio of $W_1 : O$ (v : v%) at 20,000 rpm for 6 min. The aqueous solutions of Tween-80 at three different concentrations (0.5, 1, and 1.5 v%) were the W_2 phase. In the second stage the W_1/O emulsion was re-emulsified in the W_2 aqueous phase at the three selected ratios of $W_1/O : W_2$ (10 : 90, 20 : 80, and 30 : 70 v : v%) using the above homogenizer, considering three different time and speed of homogenization (Table 1). The $W_1/O/W_2$ emulsions characteristics in terms of emulsion stability (ES) and apparent viscosity (μ_{app}) were evaluated on the basis of the four independent variables: the W_1/O to the W_2 continuous phase, the amount of Tween-80, and the homogenization time and speed (Table 1).

3. DOE and Data Analysis

The $W_1/O : W_2$ ratio (x_1), amount of Tween-80 emulsifier (x_2), time, and speed of homogenization (x_3 and x_4) were the four experimental factors selected in the present work. These controllable variables considerably affect the emulsion properties including its flow behavior. RSM with a central composite design (CCD) in the form of 2^4 full factorial design was used, where the total number of experimental runs was based on $n=2^k+2k+m$ ('k' as the number of the factors and 'm' as the repeat experiments at the center point of the design) [19,20]. Because the face-centered-design only uses three levels of each test factors [19], this design was used in the present study (FCCCD). The factor levels for experimental design were chosen based on the results obtained after optimizing the values of each factor of the $W_1/O/W_2$ double emulsion by a one-factor-at-a-time method, as shown in Fig. 1 in the results and discussion section.

Table 1 shows the arrangement of the FCCCD used in the present study. This design is suitable for exploration of quadratic response

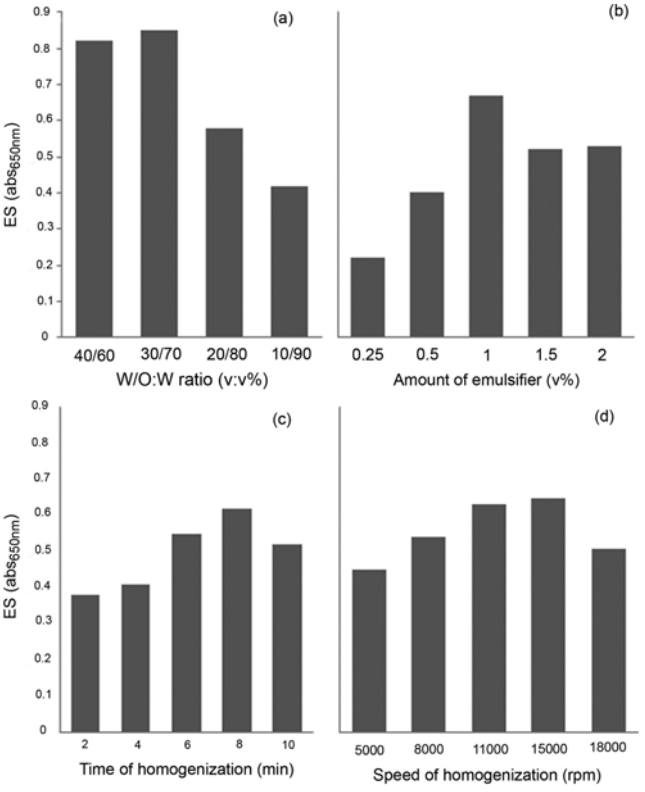

Fig. 1. Influential factors on the stability of $W_1/O/W_2$ emulsions: $W_1/O : W_2$ ratio (a), Tween-80 concentration (b), and time and speed of homogenization (c) and (d). The one-factor-at-a-time procedure has been used for obtaining the factor levels for the statistical analysis.

surface and allows development of a second-order polynomial model as follows (Eq. (1)):

$$y_i = \beta_O + \sum \beta_i x_i + \sum \beta_{ii} x_i^2 + \sum\sum \beta_{ij} x_i x_j + \varepsilon \quad (1)$$

where y_i is the predicted response, βs are the polynomial coefficients, and x_i and x_j represent coded levels of the test variables and their interactions. The coefficients in the above equation were calculated by multiple regression analysis on the experimentally obtained data, and then the predicted level of y_i was estimated ($\hat{y}_1$ emulsion stability "ES" or $\hat{y}_2$ apparent viscosity "μ_{app}") [19]. The Design Expert software (version 7.4) was used for regression and graphical analysis of the results [21].

4. Analytical Methods

In a study on performance of gum Arabic (hydrophilic emulsifier) in O/W emulsion, the spectrophotometric method has been used to evaluate emulsifying activity and stability of the system [22-24]. In that method, the stability is measured as a function of time equal to 24 h. Briefly, an appropriate aliquot of the test emulsion was diluted to about 0.001 v% using acetate buffer solution (0.2 M, pH 4.2-4.4). The diluted emulsion sample was poured into a cuvette and the absorbance was read (650 nm) after storage of the test sample for 24 h at room temperature (emulsion stability "ES").

With a polarized microscope equipped with a camera (Leica DMRX, Leica, Wetzlar, Germany), the morphology of the emulsion droplets was obtained.

The droplet size distribution of the test $W_1/O/W_2$ emulsions and the average droplet diameter were determined using a Mastersizer 2000S (Malvern Instruments, Malvern, UK) at ambient temperature according to the details given elsewhere [13].

Table 2. Statistics summaries: Comparisons of model adequacies between three equations in terms of standard deviation and coefficient of determination

Model	$\hat{y}_1$			$\hat{y}_2$		
	SD	R^2	Prob>F	SD	R^2	Prob>F
Linear	0.11	0.6996	<0.0001	0.69	0.4260	0.0061
2FI	0.1	0.8212	<0.0001	0.43	0.8293	<0.0001
Quadratic	0.021	0.9940	<0.0001	0.21	0.9685	<0.0001

Table 3. Analysis of variance (ANOVA) for the response surface reduced quadratic models developed in the present study (a), some statistical parameters obtained from the ANOVA technique are also shown (b)

(a)

Source of variation	y_1					y_2				
	Sum of squares	df	Mean square	F-value	p-value	Sum of squares	df	Mean square	F-value	p-value
Model	1.08	9	0.12	191.97	<0.0001	19.88	10	1.99	43.99	<0.0001
x_1	0.72	1	0.72	1155.7	<0.0001	6.18	1	6.18	136.82	<0.0001
x_2	0.02	1	0.02	31.98	<0.0001	0.31	1	0.31	6.79	<0.0174
x_3	4.481E-3	1	4.481E-3	7.19	<0.0144	0.97	1	0.97	21.38	<0.0002
x_4	0.017	1	0.017	27.75	<0.0001	1.38	1	1.38	30.49	<0.0001
$x_1 x_2$	0.020	1	0.020	32.01	<0.0001	0.46	1	0.46	10.23	<0.0047
$x_1 x_3$	-	-	-	-	-	5.57	1	5.57	123.24	<0.0001
$x_1 x_4$	0.034	1	0.034	54.17	<0.0001	-	-	-	-	-
$x_2 x_3$	-	-	-	-	-	0.38	1	0.38	8.37	<0.0093
$x_2 x_4$	6.765E-3	1	6.765E-3	10.85	<0.0036	-	-	-	-	-
$x_3 x_4$	0.068	1	0.068	109.07	<0.0001	1.80	1	1.80	39.73	<0.0001
x_1^2	-	-	-	-	-	-	-	-	-	-
x_2^2	0.19	1	0.19	298.99	<0.0001	2.11	1	2.11	46.72	<0.0001
x_3^2	-	-	-	-	-	0.21	1	0.21	4.65	<0.0440
x_4^2	-	-	-	-	-	-	-	-	-	-
Residual	0.012	20	6.234E-4			0.86	19	0.045		
E_{lof}	0.01	15	6.821E-4	1.53	<0.3377	0.74	14	0.053	2.21	<0.1949
E_{pure}	2.24E-3	5	4.471E-4			0. 12	5	0.024		
Total	1.09	29				20.74	29			

(b)

Parameters	$\hat{y}_1$	$\hat{y}_2$
R^2	0.9886	0.9586
R^2_{adj}	0.9834	0.9368
CV (%)	4.42	9.4
PRESS	0.036	2.6
Adequate precision	48.855	22.64

Table 4. The regression models (coded levels) for ES and μ_{app}

Response	Quadratic models
ES	$\hat{y}_1=0.66-0.2\ X_1+0.033\ X_2-0.016\ X_3+0.031\ X_4-0.16\ X_2^2-0.035\ X_{12}-0.046\ X_{14}+0.021\ X_{24}+0.065\ X_{34}$
μ_{app}	$\hat{y}_2=1.94-0.59\ X_1-0.13\ X_2+0.23\ X_3+0.28\ X_4+0.78\ X_2^2-0.25\ X_3^2+0.17\ X_{12}-0.59\ X_{13}+0.15\ X_{23}-0.33\ X_{34}$

The rheological measurements were carried out using a Paar-Physica controlled stress rotational rheometer (model MCR 300, PaarPhysica, Stuttgart, Baden-Württemberg, Germany) with a concentric cylinder geometry measuring system. This instrument was used for measuring the viscosity of the $W_1/O/W_2$ emulsions and the viscoelasticity characteristics. The viscosity data versus shear rate were obtained over the test range of the shear rate and the oscillatory rheological measurements were made when the frequency ranged from 0.05 to 100 (1/s). Linear viscoelasticity region was determined through stress sweep tests at frequency fixed at 10 Hz.

RESULTS AND DISCUSSION

1. Screening Experiments

In the present study and in characterization of $W_1/O/W_2$ emulsion in terms of the stability and the apparent viscosity, the four test factors were considered to be influential: $W_1/O : W_2$ ratio, Tween-80 concentration, time of homogenization, and speed of homogenizer, and screening experiments were carried out using one-factor-at-a-time method. In this widely practiced procedure for testing the effect of one factor, the other test factors are held constant at some pre-determined values, the findings are shown in Fig. 1. The levels of each factor were thus selected. For instance, to consider the effect of primary emulsion to continuous phase ratio, the levels of $W_1/O : W_2$ at 30 : 70 and 10 : 90 gave the highest and lowest level of ES response (1 and –1 as the coded level), respectively. Similar approach has been used for selecting the levels for the other three independent variables (Table 1(a)).

2. Model Fitting by DOE

To optimize the $W_1/O/W_2$ double emulsions stability (y_1) and the apparent viscosity (y_2) based on RSM/FCCCD, 30 experimental runs were done in the present study with different combinations of the four factors (Table 1). Table 1(b) shows responses measured experimentally for this list of 30 runs along with the predicted results obtained from the regression equations. The point in this study was to use a statistical modeling technique to obtain an empirical mathematical equation able to reproduce the experimental data. Adequacy of the quadratic equation was determined by comparing the standard deviation (SD) and the coefficient of determination (R^2) values of the three selected models: linear, 2-factor interactions (2FI), and quadratic (Table 2). The regression data obtained from the relevant ANOVA test showed that the quadratic models were adequate among the three models tested: SD_{ES}=0.021, $SD_{\mu app}$=0.21, R^2_{ES}= 0.9940, and $R^2_{\mu app}$=0.9685. Thus, the experimentally determined data for y_1 and y_2 were treated according to Eq. (1), and the results were further analyzed by ANOVA and only the terms found statistically significant by the F-test at the 5% confidence level (prob>F< 0.05) were included in the developed model(s) (Table 3(a)). Some statistical parameters obtained from the ANOVA technique are also presented in the table (Table 3(b)). Coefficient of determination decreases as a regressor variable is removed from the suggested model; thus 'adjusted R^2' which takes the number of regressor variables into account is usually selected instead of R^2 (Table 3(b)). Then according to the values of these R^2s, about more than 95% of the variations in the ES and μ_{app} results were explainable with use of the selected regressors and only less than 4% of the total variations in these responses were not explainable by the suggested models. Table 4 shows four main effects and some squared and joints effects of test factors which were significant model terms. Repeat experiments at the center point of the design are used to compute the sum squares of errors (or residuals in ANOVA table), which can be partitioned into two components: pure error (E_P) and lack-of-fit error (E_{lof}) and in the case of non-significant "lof", F-statistic indicates the developed equation is manageable in describing the obtained results, i.e., all the variations seen in the responses are due to the regressor variables included in the model (Table 3(a)) [19]. Then, the predicted values of the ES and μ_{app} responses according to the reduced quadratic polynomial equations (Tables 3(a) and 4) were compared with the experimentally measured values and the findings were indicative of reasonably close agreement between the predicted and observed data (data are not shown). At the same time, the coefficient of variation (CV%), as the ratio of the standard deviation to the mean value of the response, was equal to 4.42 and 9.4 for ES and μ_{app}, respectively, showing the standard deviation values obtained for these responses were only 4 and <10% as large as the mean level of the corresponding response (Table 3(b)). The adequate precision value, which is a measure of the signal-to-noise ratio was found to be >4, indicative of the model's navigation capability in the design space defined by the FCCCD (Table 3(b)).

Plot of the standard error of design is shown in Fig. 2, although uniformity is seen over a relatively large area of the design space, but the error increases near the boundaries. It is thus less probable to give accurate prediction of the test response considering the extreme

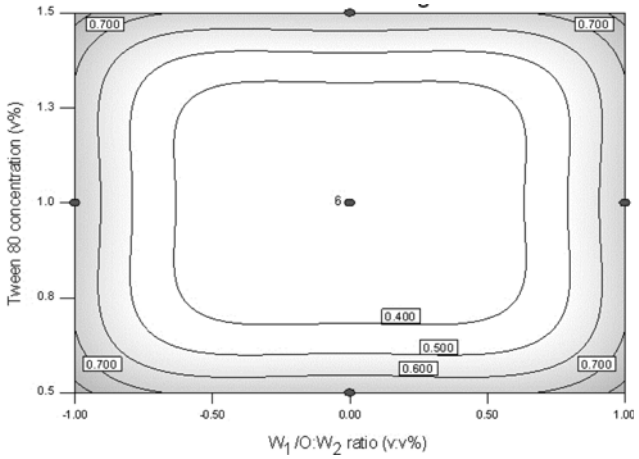

Fig. 2. Plot of standard error of design for the $W_1/O : W_2$ ratio (x_1) and the amount of Tween-80 emulsifier (x_2) in the case of the model suggested for the emulsion stability ($\hat{y}_1$).

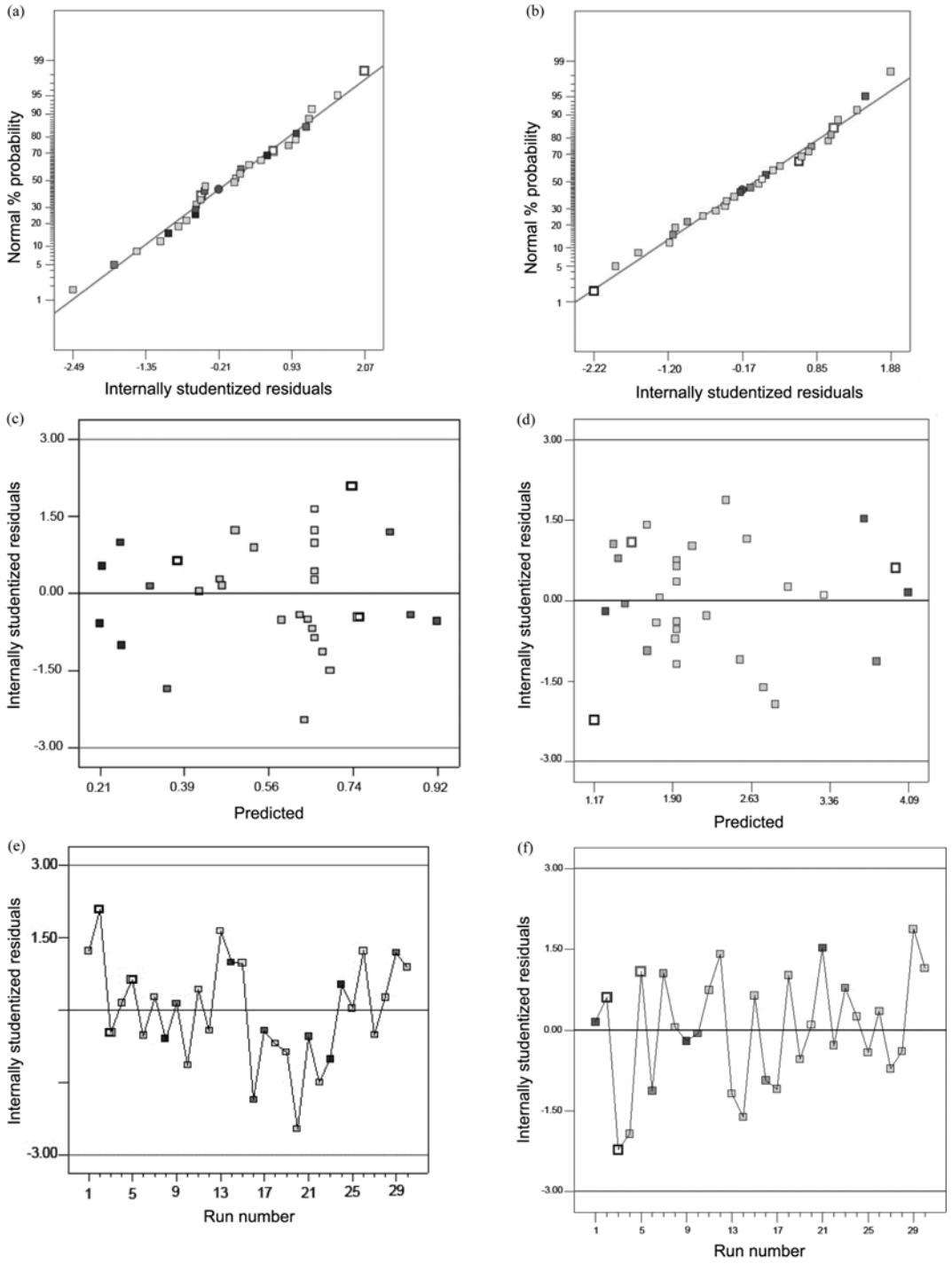

Fig. 3. Normal probability plot of the residuals for the ES (a) and the μ_{app} (b). Plots of residuals versus predicted for the ES (c) and the μ_{app} (d) are shown. Plots of residuals versus the order of the data for the ES (e) and μ_{app} (f) are also presented.

values of the selected predictors close to the boundaries of these factors.

Mathematical description for the experimental data are usually analyzed using some graphical techniques in which the assumptions of randomness, normality, independence, and constant variance can simply be checked, and it is possible to graphically detect the model failure. Fig. 3 shows the developed models were adequate in estimating experimental data within the defined range of the values of the test factors used in the present study.

The response surface diagrams of the predicted models are presented in Fig. 4. The plots are useful to visualize the joint effects of the selected factors on the test response of the ES and the μ_{app} of the $W_1/O/W_2$ emulsions, where time of homogenization and speed of homogenizer were kept constant at 6 min and 11,500 rpm, respectively. These three-dimensional plots (4(a) and 4(b)) show the ascending and descending profile, of course with different magnitude for the

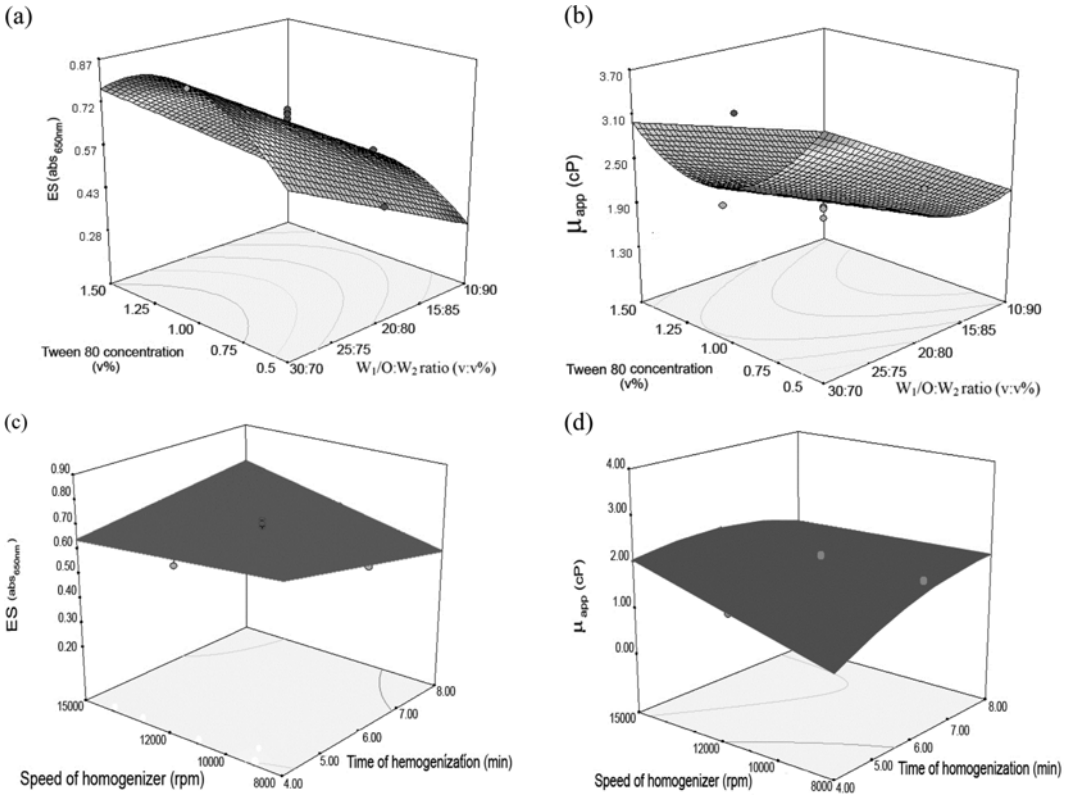

Fig. 4. Dependence of ES and μ_{app} of samples on $W_1/O : W_2$ ratio (x_1) and Tween-80 concentration (x_2) prepared at homogenization time (x_3) of 6 min and speed of homogenizer (x_4) of 11500 rpm (a) and (b). Dependence of ES and μ_{app} on x_3 and x_4 variables are also shown (c) and (d) where, the emulsions were prepared at $W_1/O : W_2$ ratio of 20 : 80 (v : v%) and Tween-80 concentration of 1 (v%).

ES and μ_{app} responses. As it is seen, the maximum ES was achieved with Tween-80 concentration (x_2) at about the center point when $W_1/O : W_2$ (x_1) ratio was at its lowest level. With further decrease in concentration of the hydrophilic test emulsifier, a noticeable reduction in the emulsion stability occurs at any point along the line of $W_1/O : W_2$ (x_1) ratio. Apparently, Tween-80 at the test level equal to 1 (v%) performed efficiently in providing protective interfacial layer to keep the $W_1/O/W_2$ double emulsion stable when the amount of primary emulsion was high ($W_1/O : W_2$ ratio equal to 30 : 70). It is important to keep Tween-80 at the defined minimum level since Tween-80 at high concentration in $W_1/O/W_2$ preparation, could solubilize hydrophobic type of surfactant (Span-80) and this oily emulsifier becomes less available for stabilization of W_1/O primary emulsion; consequently, $W_1/O/W_2$ double emulsion stability decreases [7,25]. The positive effect of Tween-80 (x_2) and the negative effect of $W_1/O : W_2$ ratio (x_1) and of the interaction between x_1 and x_2 on the ES, as shown by the suggested mathematical model (Table 4), indicated that a simultaneous increase in Tween-80 concentration and $W_1/O : W_2$ ratio (i.e., the coded value of the ratio of 30 : 70 equals to −1) leads to an increase in the ES response (Fig. 4(a)).

The surface plots for the viscosity response are also shown in Fig. 4. The descending profile of the μ_{app} shows the highest level of this response was at the highest concentration of Tween-80 emulsifier and of the $W_1/O : W_2$ ratio (the coded value of highest Tween-80 concentration equals to 1 and the coded value of 30 : 70 volume ratio equals to −1) (Table 1(a)). The μ_{app} reaches to its minimum level at the emulsifier concentration at the center point at $W_1/O : W_2$ ratio at the highest level (i.e., the coded value of 10 : 90 $W_1/O : W_2$ ratio equals to 1), thereafter, the μ_{app} increases with decrease in level of the test emulsifier. The negative effect of $W_1/O : W_2$ ratio (x_1) and of the Tween-80 concentration (x_2) and the positive effect of interaction between these two test factors on the μ_{app} (Table 4) indicated that a simultaneous decrease in x_1 and x_2 resulted to an increase in the $W_1/O/W_2$ viscosity (Fig. 4(b)).

In monitoring the viscosity response, the extent of decreasing trend of $W_1/O : W_2$ ratio (x_1) was visually lower as compared to that which is seen for x_1 in the ES surface plot (Fig. 4(a) and (b)). For instance, in double emulsions viscosity, changes frequently are related to water movement from inner aqueous phase to the outer continuous aqueous phase or vice versa, and weakness of the formed film on the interface was found to be a reason for the water passage between the phases [7]. Study on the modified pectin hydrocolloid and whey protein isolate in the preparation of the $W_1/O/W_2$ emulsions showed that increasing the rigidity of the formed film at the interface positively affected the emulsion stabilization. The behavior was found to be the result of water transport prevention, and system's low viscosity extended the emulsion stability [26]. The type and concentration of secondary emulsifier on the $W_1/O/W_2$ emulsions have also been discussed in the literature [5,8,15]. With considering these points, at a certain ratio of the $W_1/O : W_2$, stabilization of the hydrophobic primary emulsifier increased at high concentrations of the secondary emulsifier (Tween-80) and low water movement was the result of keeping Tween-80 at the minimum level; thus more of the primary emulsifier was available for the W_1/O sta-

Table 5. Optimization criteria used in the present study (a). Optimal solutions (predicted values) obtained by the design expert based on the first criterion (b) and the second criterion (c) are also shown

(a)

Independent/ dependent variables	Limits*		Importance	First criterion$_1$	Second criterion$_2$
	Lower	Upper			
x_1 (v/v %)	−1	+1	3	Is in range	Minimize
x_2 (v %)	−1	+1	3	Is in range	Is in range
x_3 (min)	−1	+1	3	Minimize	Minimize
x_4 (rpm)	−1	+1	3	Minimize	Minimize
y_1 (abs 650 nm)	0.202	0.907	5	Maximize	Maximize
y_2 (cP)	0.85	4.11	3	Is in range	Is in range

(b)

Exp. no	x_1	x_2	x_3	x_4	$\hat{y}_1$	$\hat{y}_2$	Desirability
1	−1	−0.01	−1	−1	0.87	0.85	0.972
2	−1	−0.02	−1	−1	0.87	0.85	0.972
3	−1	0.02	−1	−0.98	0.87	0.85	0.971
4	−0.98	−0.01	−1	−1	0.86	0.85	0.971
5	−1	0.09	−0.98	−1	0.87	0.85	0.971

(c)

Exp. no	x_1	x_2	x_3	x_4	$\hat{y}_1$	$\hat{y}_2$	Desirability
1	−1	0.01	−0.99	−1	0.87	0.85	0.978
2	−1	0	−1	−0.99	0.87	0.85	0.978
3	−1	0.07	−0.98	−1	0.87	0.85	0.977
4	−1	0.15	−0.97	−0.99	0.87	0.85	0.975
5	−1	0.17	−0.96	−1	0.87	0.85	0.975
6	−1	0.17	−1	−0.90	0.87	0.85	0.970

*The limits for x variations are in coded levels while the actual values are used for the responses

bilization [25].

Effects of variations of the time of homogenization and the speed of homogenizer on the ES and μ_{app} were also examined. Effects of these independent variables at the constant $W_1/O : W_2$ ratio equal 20 : 80 (v : v%) and the Tween-80 concentration of 1 (v%) on the ES were negligible (Fig. 4(c)). A linear relationship between μ_{app}, time of homogenization, and speed of homogenizer is also seen in Fig. 4(d).

The optimal $W_1/O/W_2$ emulsion characteristics in terms of the stability and the apparent viscosity were determined through the reduced regression models (Table 4) using the function of desirability as described by the Design Expert software. Two criteria in the present work were applied to maximize the ES while the μ_{app} could be maintained within the experimental range (i.e., because of importance of the ES response, this variable was kept higher in the first criterion when $W_1/O : W_2$ (x_1) was within the test range). Table 5 summarizes these two criteria and the optimal solutions given by the software. The accuracy of the predicted models was validated by performing four experiments using the conditions given in Table 5(b) and 5(c). With use of the predicted values of the test factors, the ES and μ_{app} were experimentally determined and the results were in good agreement with the predicted values (according to the suggested models) and relatively small errors were between these values (Table 6).

3. Rheological Studies

Based on the dispersed phase content, emulsions can be divided into two groups: the emulsions exhibiting Newtonian fluid character which are those having low concentration of the dispersed phase

Table 6. Validation of the test results

Experimental run numbers	x_1	x_2	x_3	x_4	Responses					
					Observed values		Predicted values		Error %	
					y_1	y_2	$\hat{y}_1$	$\hat{y}_2$	y_1	y_2
0	−1	0	−1	−1	0.82	0.92	0.87	0.85	5.7	8.2
1	−1	0.17	−1	−1	0.84	0.91	0.87	0.85	3.4	7
2	−0.87	0.56	−1	−1	0.81	0.88	0.87	0.85	6.9	3.5
3	−1	0.12	−1	−0.6	0.91	0.89	0.87	0.85	4.6	4.7

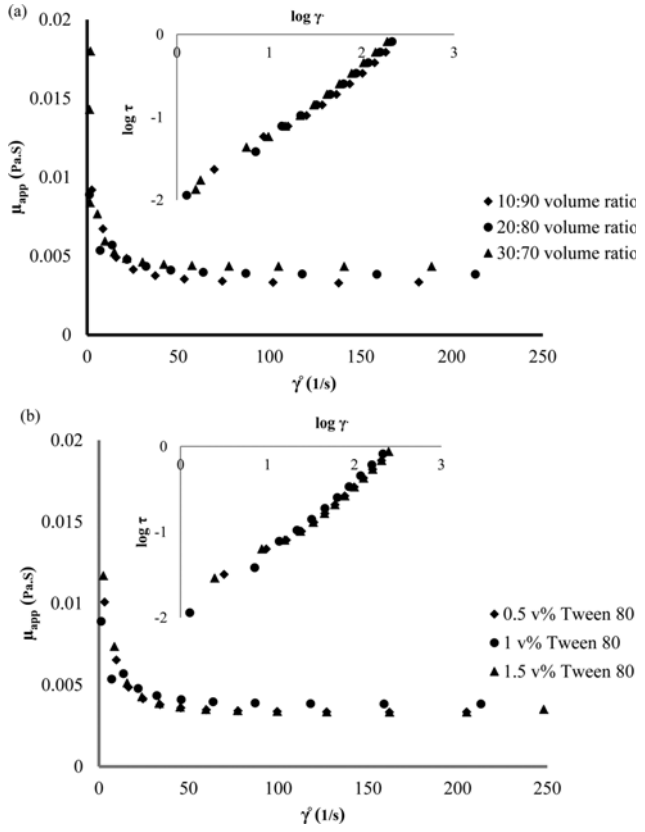

Fig. 5. Apparent viscosity against shear rate for the test emulsions of the $W_1/O/W_2$ prepared with different $W_1/O : W_2$ ratios (a) and different concentrations of Tween-80 (b). Insert is the log-log plot of shear stress against shear rate for determining the consistency index from the intercept on the y axis and the flow behavior index from the slope.

(independency of viscosity on the shear rate), while the emulsions with high concentration of dispersed phase exhibit non-Newtonian fluid characteristic [27]. Steady state rheological measurements in the form of the functional relationship between shear stress (τ, 'Pa') and shear rate ($\dot{\gamma}$, '1/s') of the $W_1/O/W_2$ emulsions shown in Fig. 5 (log-log plot "insert") reveal that the emulsions exhibited non-Newtonian flow character. The flow curves in the 'insert' are linear indicating pseudoplastic behavior [28]. In the present study, a power law equation (Eq. (2)) was used for describing quantitative relation between apparent viscosity (μ_{app}, 'Pa·s') of the test emulsions and the shear rate [29,30]:

$$\mu_{app} = \frac{\tau}{\dot{\gamma}} = k\dot{\gamma}^{n-1} \tag{2}$$

where k is the consistency index (Pa·s^n) and n as the dimensionless constant is called the flow behavior index.

The values of flow behavior indices and the consistency coefficients with the R^2, and RMSE of the test $W_1/O/W_2$ emulsions, all are given in Table 7. The two other model equations, Bingham and Casson, in describing the rheological behavior of the test $W_1/O/W_2$ emulsions have been also applied in the present study. These models were found to be effective in explaining the plasticity behavior where presence of three-dimensional networks of the aggregated emulsion droplets is critical in applying stress to the fluids, and the breakage of weak bonds in these networks may occur when the applied stress exceeds above certain level [1]. Of course, more work is needed to show involvement of Tween-80 emulsifier and the particles aggregation in forming structured networks in the test $W_1/O/W_2$ emulsions as described in the present work (Table 7).

Non-Newtonian pseudoplasticity behavior was observed for 10 : 90 and 30 : 70 $W_1/O : W_2$ ratios, where n is less than unity. The consistency index (k) indicative of the viscous nature of the system under

Table 7. Values of rheological model parameters (n, k, and τ_0) and the relevant regression coefficients for the test $W_1/O/W_2$ emulsions prepared using different amounts of the primary emulsion at the constant level of Tween 80 (a) and different concentrations of Tween 80 emulsifier at the constant level of the $W_1/O : W_2$ ratio (b)

(a)

Model	$W_1/O : W_2$ ratio (v/v%)											
	10 : 90				20 : 80				30 : 70			
	τ_0 (Pa)	k (Pa s^n)	n	R^2 (RMSE)	τ_0 (Pa)	k (Pa s^n)	n	R^2 (RMSE)	τ_0 (Pa)	k (Pa s^n)	n	R^2 (RMSE)
Casson	5×10^{-3}	51×10^{-3}	---	0.99 (0.75)	26×10^{-3}	84×10^{-3}	---	0.98 (0.14)	3×10^{-3}	60×10^{-3}	---	0.99 (0.03)
Power law	---	11×10^{-3}	0.75	0.99 (0.02)	---	5×10^{-3}	0.99	0.98 (0.01)	---	12×10^{-3}	0.75	0.97 (0.02)
Bingham	22×10^{-3}	3×10^{-3}	---	0.99 (0.03)	10×10^{-3}	4×10^{-3}	---	0.98 (0.03)	14×10^{-3}	4×10^{-3}	---	0.99 (0.04)

(b)

Model	Tween-80 concentration (v%)											
	0.5				1				1.5			
	τ_0 (Pa)	k (Pa s^n)	n	R^2 (RMSE)	τ_0 (Pa)	k (Pa s^n)	n	R^2 (RMSE)	τ_0 (Pa)	k (Pa s^n)	n	R^2 (RMSE)
Casson	5×10^{-3}	52×10^{-3}	---	0.99 (0.1)	26×10^{-3}	84×10^{-3}	---	0.98 (0.03)	5×10^{-3}	52×10^{-3}	---	0.99 (0.15)
Power law	---	11×10^{-3}	0.75	0.98 (0.08)	---	5×10^{-3}	0.99	0.98 (0.02)	---	11×10^{-3}	0.74	0.97 (0.12)
Bingham	22×10^{-3}	3×10^{-3}	---	0.99 (0.14)	4.1×10^{-1}	7×10^{-3}	---	0.98 (0.04)	18×10^{-3}	3×10^{-3}	---	0.99 (0.19)

The values of the square root of the mean squared deviations referred to as the standard deviation between experimental and predicted values of τ for each model are shown in parentheses, $\sqrt{\sum[(\tau_{exp}-\tau_{pred})/\tau_{pred}]^2/N}$($R^2$ and RMSE give a measure of the goodness of fit of the experimental data to the suggested model)

study was higher among other k values for the highest dispersed phase content of the test $W_1/O/W_2$ emulsion (30 : 70). The $W_1/O/W_2$ emulsion prepared with 1 v% Tween-80 ($W_1/O : W_2$ ratio=20 : 80) can be categorized as Newtonian fluid (n=0.99). Solutions of pure gum arabic with concentration of less than 40% exhibit Newtonian flow behavior [18]. The results of Table 7, which show change of rheological behavior between Newtonian and non-Newtonian flow, are in agreement with the findings reported in the literature, such as cases where O/W emulsions were prepared with use of whey protein and gum arabic as the emulsifier [28].

Fig. 5(a) shows the apparent viscosity as function of shear rate where three different $W_1/O : W_2$ ratios with Tween-80 emulsifier at the constant level of 1 v% have been used for emulsion preparation and $W_1/O : W_2$ ratio at 30 : 70 gave the highest μ_{app}. The decreasing trend of μ_{app} can also be seen in this figure, where the viscosity by reaching to shear rate equal to 50 1/s remained relatively constant. The extent of viscosity decrease was higher for the higher level of the dispersed phase compared with the decreasing degree of the μ_{app} for the other two test dispersed to continuous phase ratios (Fig. 5(a)). Similar trend is also seen in Fig. 5(b) where three levels of the Tween-80 emulsifier each with the constant $W_1/O : W_2$ ratio (at 20 : 80) were used in preparation of the test emulsions. The amounts of water in the outer aqueous phase affects the extent of emulsion droplets entanglement, i.e., the more water that exists in the outer aqueous phase, the more apart are the neighboring particles from each other, and viscosity as a measure of this relation thus would be decreased as seen in Fig. 5(a).

Penetration of core materials through the oil layer to the external W_2 phase and subsequent back diffusion of water from the inner aqueous phase to the W_2 phase resulted in viscosity decrease, as it is shown in the study on the time dependency of the $W_1/O/W_2$ emulsion [7,25,26]. These types of observations are attributable to water pas-

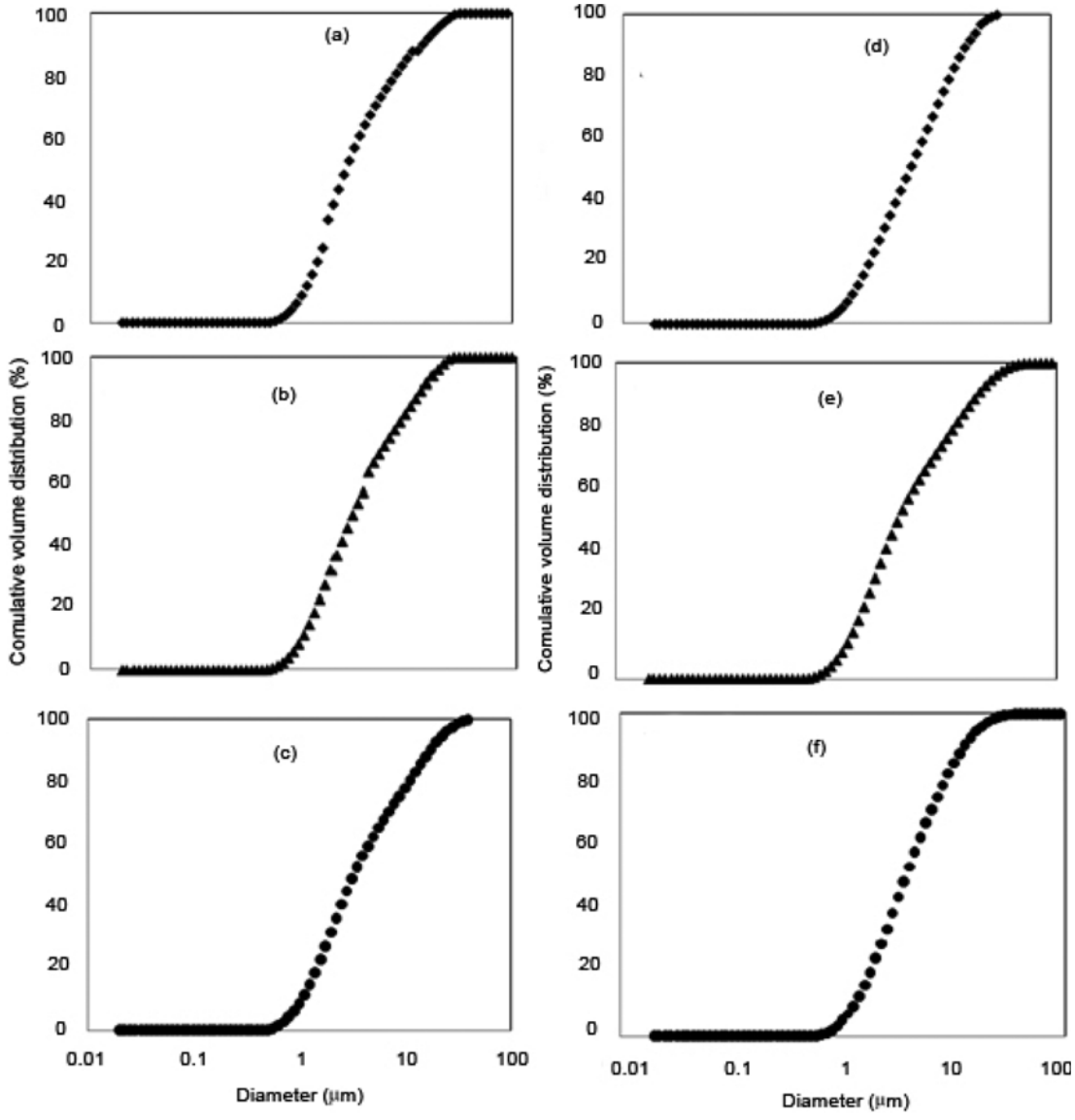

Fig. 6. Cumulative particle size distribution of the test $W_1/O/W_2$ emulsions: W_1/O (10) : W_2 (90) ratio (v : v%) (a), W_1/O (20) : W_2 (80) ratio (v : v%) (b), W_1/O (30) : W_2 (70) ratio (v : v%) (c), Tween-80 concentration 0.5 (v%) (d), Tween-80 concentration 1 (v%) (e), Tween-80 concentration 1.5 (v%) (f).

sage between phases, the colloidal nature of these phases, and emulsion particle size distribution.

The nature of the emulsifier film formed at the interface and the strength of this layer are also critical, mainly because of specific role of emulsifier in making efficient adsorbed layer, i.e., prevention of water passages.

Further study was focused on particle size determination, and Fig. 6 shows the size distribution pattern for each of the three test emulsions, prepared with 10 : 90, 20 : 80, and 30 : 70 volume ratios, expressed as the cumulative function. The resulting plots appear as S-shaped curves with the emulsion droplets having relative ranges from 0.4 to 60 μm in size (Figs. 6(a), 6(b), and 6(c)). The particle size where the cumulative distribution is 50% is known as the median droplet diameter ($d_{v,0.5}$) with 50% of the particles under 2.66, 2.85, and 3.29 for the emulsions of 10 : 90, 20 : 80, and 30 : 70 volume ratios, respectively. The median droplet diameter often is the better representative value since it is an average of position of data. Cumulative plots of the three test emulsions each prepared with the specified amounts of Tween-80 are also S-shaped curves (Figs. 6(d), 6(e), and 6(f)).

Different natural hydrocolloids were examined in preparation of O/W emulsions, and the results of particle size distributions were presented as the cumulative plots (double S-shaped curves). It was found that smallest emulsion particles prepared with Fenugreek gum corresponded to the largest SSA value [31]. We concluded that Fenugreek gum gave lowest viscosity compared to that of using Xanthan gum in the emulsion preparation.

Table 8 contains the tabulated results for the particle diameter range, specific surface area (SSA), span, and volume surface mean diameter (d_{32}) for the six test emulsions.

In fact, the following expression shows importance of the interfacial area per unit volume of emulsion (A/V) and dispersed phase volume fraction (ϕ_v) in measuring the droplet mean diameter [32]: $D=6\phi_v/A$. Increase in surface area with decrease in particle size exerts a tension on the surfactant, as adequate amount of this compound should be present in the system to cover the droplet surfaces.

The data presented in Table 8 and also in Fig. 6 show the emulsions in the present study had droplets essentially of similar size. Also, the effect of non-ionic surfactant on reduction of droplet size was more effective in the O/W emulsions prepared with the mineral oil hydrocarbons than those prepared with use of olive oil (triacylglycerol) [33].

This effectiveness was related to the structural similarity between the non-ionic surfactant and the dispersed phase. The particle size range for the $W_1/O/W_2$ emulsions in the present study, which were prepared with use of the canola oil, was similar to the size ranges reported for the single type emulsions prepared with the mineral oil as the dispersed phase. Table 8 shows approximately 60% of the droplets in $W_1/O/W_2$ emulsions were in the small particle size range, less than 5 μm. The range of d_{32} was 2.3 to 2.9 μm while SSA which is inversely correlated to d_{32} was about 2.5 m^2/g.

Multiple emulsions are also known to be viscoelastic liquids and show properties of both liquids and solids; these characteristics can be quantitatively described on the basis of the results of oscillatory experiments. The complex modulus (G*) is comprised of G′ and G″ moduli, where G′ as a measure of the energy stored elastically in the material is the elastic component of the complex modulus and G″ a measure of the energy dissipated as viscous flow is the viscous component of the G* [15,16]. Fig. 7 shows the shear stress dependence of G′ (storage modulus) and G″ (loss modulus) for the $W_1/O/W_2$ test emulsions in the present study. These emulsions were prepared with use of the three different $W_1/O : W_2$ ratios at the constant level of Tween-80 emulsifier (1 v%). As it can be seen in Fig. 7, loss modulus stays above the G over the entire shear stress range, i.e., these emulsions showed viscous liquid-like behavior. The viscoelasticity measurements indicate there was no perturbation of the system's structure after obtaining the linear viscoelastic region in the curves of G′ and G″ as function of shear stress. Viscoelastic measurements were also obtained as a function of the frequency changes; and as Fig. 8 shows, the values of loss modulus stay above the elastic modulus (G″>G′), which indicates dominance of viscous liquid-like property of the emulsions. Comparison of the results presented in Fig. 7(b) shows that changes in the emulsion property are similar to those variations seen in Fig. 7(a).

Table 8. The particle size distribution of diameter range, volume surface mean diameter (d_{32}), specific surface area (SSA), and span values obtained from the size distribution data for the $W_1/O/W_2$ test emulsions, where three $W_1/O : W_2$ ratios were used in the emulsion preparation with the constant Tween-80 level (a). These specifications for the test emulsions prepared with the three levels of Tween-80 at a constant ratio of $W_1/O : W_2$ are also shown (b)

(a)

	Diameter range of 0-5 μm%	Diameter range of 5-60 μm%	Volume surface mean diameter (d_{32}) μm	Specific surface area (SSA) m^2/g	Span
10 : 90 Volume ratio	65.73	34.26	2.316	2.59	5.096
20 : 80 Volume ratio	63.1	36.9	2.4	2.5	4.98
30 : 70 Volume ratio	62.25	39.75	2.412	2.49	4.981

(b)

	Diameter range of 0-5 μm%	Diameter range of 5-60 μm%	Volume surface mean diameter (d_{32}) μm	Specific surface area (SSA) m^2/g	Span
0.5 v% Tween 80	55.02	45.98	2.477	2.42	2.987
1 v% Tween 80	63.1	36.9	2.4	2.5	4.98
1.5 v% Tween 80	65.82	34.18	2.907	2.06	3.048

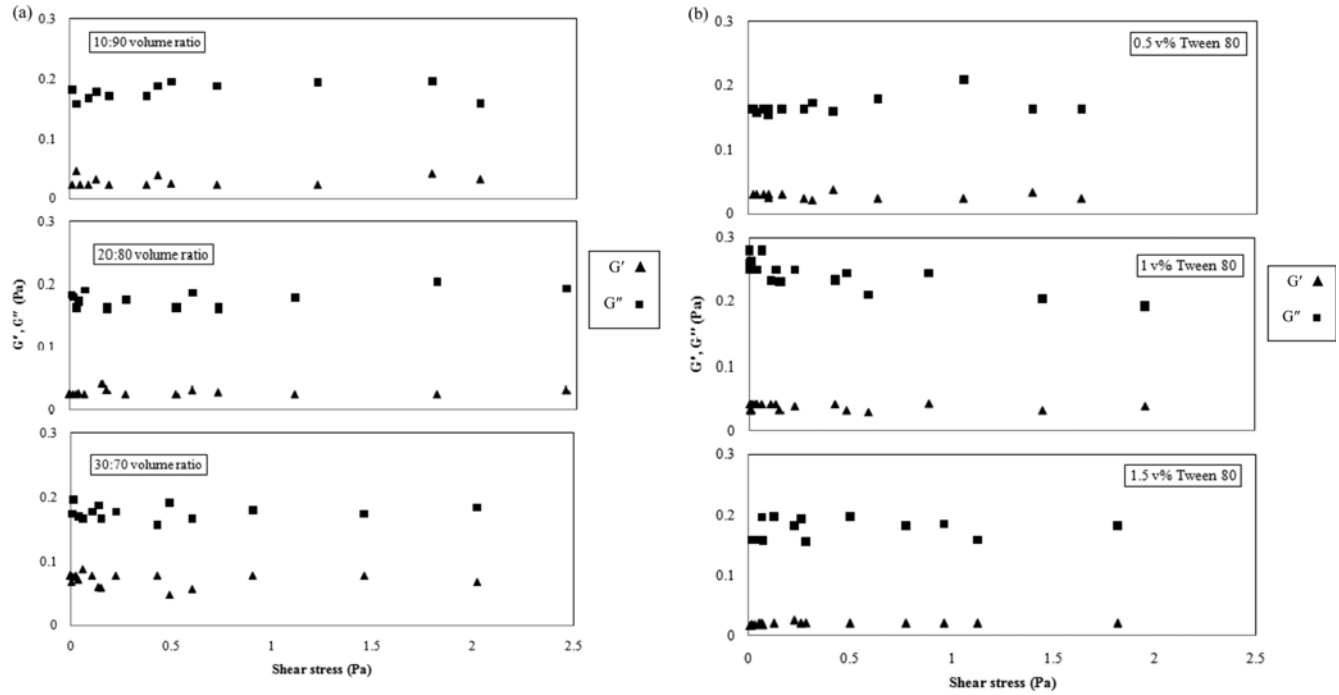

Fig. 7. Shear-stress dependence of the G′ and G″ for test $W_1/O/W_2$ emulsions.

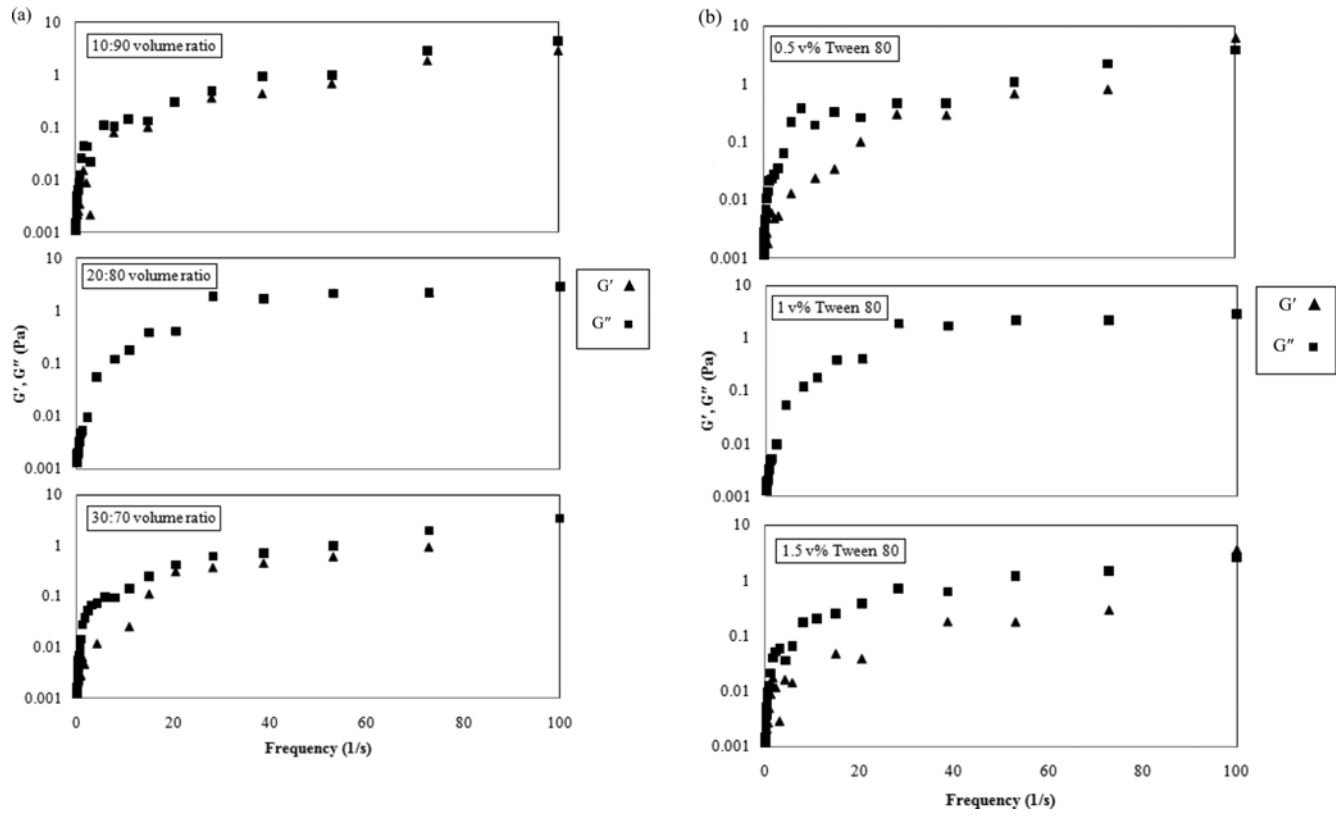

Fig. 8. Frequency dependence of the G′ and G″ for test $W_1/O/W_2$ emulsions.

CONCLUSIONS

With use of RSM and CCD, the relationships between the four selected factors used in the preparation of the $W_1/O/W_2$ emulsions containing $FeSO_4 \cdot 7H_2O$ as the inner phase were quantified and based on the regression model obtained, the emulsion formulation conditions were adequately predicted. The non-Newtonian behavior of the test $W_1/O/W_2$ emulsions was analyzed using Power law, Bing-

ham, and Casson models on the basis of R^2 and RMSE values.

According to the results of particle size distribution pattern, more than 60% of particles were less than 5 μm. Complexity of the particle interactions involved in the multiple emulsions formation is much higher compared with those of the single emulsions, and it would be reasonable to find time-dependency of the changes for the particle size distribution. A simple ANOVA test in this regard provides informative results about the emulsion stability as related to the particles morphology.

The liquid-like property of the test $W_1/O/W_2$ emulsions was found to dominate based on the oscillatory experiments results ($G' < G''$).

Human diet deficiency in iron intake is a worldwide problem and availability of different methods of encapsulation actually is based on the separation of this oxidatively sensitive microelement from other food items. Double emulsion and its rheological characterization could be an essential part of the microencapsulation technology.

NOMENCLATURE

CV : coefficient of variation [%]
df : degree of freedom
D : median droplet diameter [μm]
d_{32} : volume surface mean diameter [μm]
E_{lof} : lack-of-fit error
E_{pure} : pure error
ES : emulsion stability [$abs_{650\ nm}$]
G* : complex modulus [Pa]
G' : storage modulus [Pa]
G'' : viscous modulus [Pa]
K : consistency index [Pa s^n]
n : flow behavior index
R^2 : coefficient of determination
SD : standard deviation
SSA : specific surface area [m^2/g]
x_1 : $W_1/O : W_2$ ratio [v : v%]
x_2 : Tween-80 concentration [v%]
x_3 : time of homogenization [min]
x_4 : speed of homogenizer [rpm]
y_1 : emulsion stability response [$abs_{650\ nm}$]
y_2 : apparent viscosity response [cP]
$\hat{y}_1^*$: emulsion stability predicted response [$abs_{650\ nm}$]
$\hat{y}_2^*$: apparent viscosity predicted response [cP]
2FI : 2-factor interactions
β_0 : coefficient for constant value
β_1 : coefficient for $W_1/O : W_2$ ratio
β_2 : coefficient for Tween-80 concentration
β_3 : coefficient for time of homogenizer
β_4 : coefficient for speed of homogenizer
β_{22} : coefficient for (Tween-80 concentration)^2
β_{33} : coefficient for (time of homogenizer)^2
β_{12} : coefficient for ($W_1/O : W_2$...) (Tween-80...)
β_{13} : coefficient for ($W_1/O : W_2$...) (Time…)
β_{14} : coefficient for ($W_1/O : W_2$...) (Speed…)
β_{23} : coefficient for (Tween-80...) (Time…)
β_{24} : coefficient for (Tween-80...) (Speed…)
β_{34} : coefficient for (Time…) (Speed…)
$\dot{\gamma}$: shear rate [1/s]
μ_{app} : apparent viscosity [cP]
τ : shear stress [Pa]

REFERENCES

1. D. J. McClements, *Food emulsions: Principles, practices, and techniques*, CRC Press, Boca Raton Fl (2005).
2. F. Nazzaro, P. Orlando and F. Fratianni, *Curr. Opin. Biotechnol.*, **23**, 182 (2012).
3. F. J. Colmenero, *Food Res. Int.*, **52**, 64 (2013).
4. A. K. Anal and H. Singh, *Trends Food Sci. Technol.*, **18**, 240 (2007).
5. N. Garti, *Lebensm-Wiss Technol.*, **30**, 222 (1997).
6. J. L. Salager, R. E. Anton, D. A. Sabatini, J. H. Harwell, E. J. Acosta and L. I. Tolosa, *J. Surfactants Deterg.*, **8**, 3 (2005).
7. T. Schmidt, D. Dobler, A. Guldan, N. Paulus and F. Runkel, *Colloids Surf., A.*, **372**, 48 (2010).
8. Sh. Magdassi, M. Frenkel, N. Garti and R. Kasan, *J. Colloid Interface Sci.*, **97**(2), 374 (1984).
9. S. R. Derkatch, S. M. Levachov, A. N. Kuhkushkina, N. V. Novosyolova, A. E. Kharlov and V. N. Matveenko, *Colloids Surf., A.*, **298**, 225 (2007).
10. E. Dickinson and S. T. Hong, *Colloids Surf., A.*, **127**, 1 (1997).
11. B. P. Binks and S. O. Lumsdon, *Langmuir*, **17**, 4540 (2001).
12. M. Inoue, K. Hashizaki and H. Taguchi, Y. Saito, *Chem. Pharm. Bull.*, **56**(5), 668 (2008).
13. L. Davarpanah and F. Vahabzadeh, *Starch/Starke*, **64**, 898 (2012).
14. L. Davarpanah, F. Vahabzadeh and A. Dermanaki, *Oil Gas Sci. Technol.*, (2013), DOI:10.2516/ogst/2012066.
15. I. Terrisse, M. Seiller, A. Rabaron and J. L. Grossiord, *Int. J. Cosmetic. Sci.*, **15**, 53 (1993).
16. THF. Tadros, *Colloids Surf., A.*, **91**, 39 (1994).
17. M. M. Murillo-Martinez, R. Pedroza-Islas, C. Lobato-Calleros, A. Martinez-Ferez and E. J. Vernon-Carter, *Food Hydrocoll.*, **25**, 577 (2011).
18. O. R. Fennema, *Food Chemistry*, Marcel Dekker NY (1985).
19. R. H. Myers and D. C. Montgomery, *Response surface methodology process and product optimization using designed experiments*, Wiley, NY (2002).
20. L. L. Lapin, Modern Engineering Statistics, Wards-worth Publishing Company, Belmont, CA, USA (1997).
21. http://www.statease.com/dx8_man.html.
22. Y. Kim, C. Morr and T. Schenz, *J. Agric. Food Chem.*, **44**, 1308 (1996).
23. T. Aoki, A. E. Decker and D. J. McClements, *Food Hydrocoll.*, **19**, 209 (2005).
24. M. P. Yadav, M. Igartuburu, Y. Yan and E. A. Nothnagel, *Food Hydrocoll.*, **21**, 297 (2007).
25. J. Jiao and D. J. Burgess, *AAPS PharmSci.*, **5**(1) Article 7, (2003) (http://www.pharmsci.org).
26. R. Lutz, A. Aserin, L. Wicker and N. Garti, *Colloids Surf., B.*, **72**, 121 (2009).
27. L. G. Torres, R. Iturbe, M. J. Snowden, B. Z. Chowdhry and S. A. Leharne, *Colloids Surf., A.*, **302**, 439 (2007).
28. E. Ibanoglu, *J. Food Eng.*, **52**, 273 (2002).
29. R. Toledo, *Fundamentals of food process engineering*, van Nostrand Reinhold: NY (1991).

30. P. M. Doran, *Bioprocess engineering principles*, Academic Press (1995).
31. X. Huang, Y. Kakuda and W. Cui, *Food Hydrocoll.*, **15**, 533 (2001).
32. J. Frelichowska, M. A. Bolzinger and Y. Chevalier, *J. Colloid Interface Sci.*, **351**, 348 (2010).
33. R. P. Gullapalli and B. B. Sheth, *Eur. J. Pharm. Biopharm.*, **48**, 233 (1999).